ACTIVE NEGATIVE INDUCTOR BASED ON MAGNETIC FLUX

D. D. Stancil[*]

Department of Electrical and Computer Engineering, North Carolina State University, Raleigh, NC 27695, USA

Abstract—An active circuit is described that exhibits the equivalent reactance of a negative inductor. In contrast with previous techniques based on negative impedance converters, the negative inductance is produced by generating an opposing time-varying magnetic flux. The new circuit also enables the inductance to be electronically varied between negative and positive values, can enhance the Q, and defaults to a conventional positive inductor in the event of active component failure. The performance of a prototype with an inductance of $-0.344\,\mathrm{mH}$ and operating over the frequency range 1–40 kHz is described.

1. INTRODUCTION

The bandwidth of matching circuits using lumped components is limited by the fact that the frequency dependences of inductive and capacitive reactances are different. One way to overcome this difficulty is to use negative inductors and capacitors. By this we mean components that have the same frequency dependence but the opposite signs to those of ordinary inductors and capacitors. Such components violate Foster's Reactance Theorem [1] and require active elements for their realization. Negative Impedance Converter (NIC) circuits have been known since the early 1950s [2, 3]. A listing of 12 two-port floating (i.e., input and output ports do not share a common terminal) NICs realized with two transistors has been given by Kuo and Su [4], and 10 different common terminal transistor NICs have been catalogued by Sussman-Fort [5]. NICs using op-amps have also been described in the literature [6]. A thorough discussion of the use of non-Foster circuits to match antennas has been presented by Sussman-Fort and Rudish [7].

* Corresponding author: Daniel D. Stancil (ddstancil@ncsu.edu).

All of these NICs use circuit techniques to invert the voltage or current across an impedance element, thus realizing the negative of the element impedance. These techniques are independent of the element, and can be used with resistors, capacitors, and inductors.

In contrast, the negative inductor that is presented here is based on modifying the magnetic flux linkage in a physical inductor, and is closer in principle to recently reported active magnetic metamaterials [8] or tunable inductors [9–12]. In the magnetic metamaterial [8], a current is induced in an input loop by an applied time-varying magnetic field, and this current is amplified, inverted, and applied to a parallel output loop a short distance away. By stacking cells of this sort, a metamaterial can be realized that exhibits an induced magnetic dipole moment density with opposite polarity to a conventional magnetic material. In a similar way, the device described here senses the current into an inductor, then amplifies the current and applies an opposing time-varying magnetic flux via a second inductor magnetically coupled to the first. If the gain is sufficiently large, the driven response can overcome the natural response of the inductor, leading to negative inductance values. Pehlke et al. [9] introduced a high-Q tunable inductor based on a similar principle, and tunable inductors using this idea have been discussed by a number of authors [9–12]. However, these authors do not discuss the possibility of achieving negative inductance values.

Although not as versatile as a conventional NIC (i.e., it is applicable only to inductors in its present form), the new device does have other attractive features such as the ability to vary the effective inductance continuously over negative to enhanced-positive values, and graceful degradation in the event of an active component failure. This latter attribute follows from the fact that the terminal current does not flow directly through any active device. Consequently, if an active device fails, one is simply left with a conventional passive (positive) inductor.

2. DEVICE CONCEPT

To introduce the concept, first consider the circuit shown in Figure 1(a). In this diagram, the inductors L_1 and L_2 are coupled through the mutual inductance M. It is straightforward to show that in the limit $R_2 \ll \omega L_2$ the source sees the impedance $R_{eff} + j\omega L_{eff}$, where

$$R_{eff} \approx R_1 + k^2 \frac{L_1}{L_2} R_2, \quad L_{eff} = \left(1 - k^2\right) L_1, \qquad (1)$$
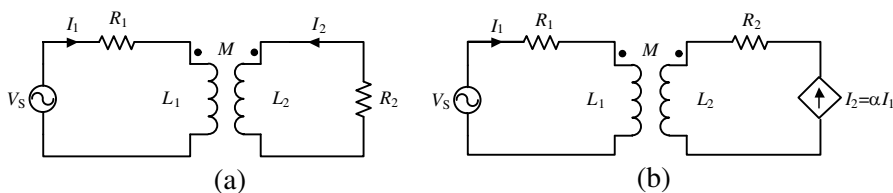
Figure 1. Circuits illustrating the device concept. (a) Currents induced in the secondary circuit reduce the inductance seen by the input loop owing to Lenz' law. (b) Addition of a dependent current source in the secondary circuit can either enhance the inductance seen by the input loop or drive it to negative values.

and k is a dimensionless coupling constant defined such that $M = k\sqrt{L_1 L_2}$. We see that the current induced in the secondary circuit has the effect of reducing the inductance seen by the source in the primary circuit. This is a consequence of Lenz' Law, i.e., a secondary current is induced that tends to oppose the variations in magnetic flux induced by the primary current. However, it is apparent that when the flux linkage is maximum (i.e., $k = 1$), the effective inductance can be reduced to zero but cannot be negative. This reduction in flux linkage is a drawback of the use of solid ground shields to isolate planar inductors from solid state substrates [13], and has been used to intentionally reduce the coupling in planar transformers [14]. Note that by putting a switch in the secondary, the inductance can be toggled between two values. This principle has been used by several research groups to realize switch-reconfigurable inductors [13–19]. Tunable inductors have also been reported that are based on changing the bias on a magnetic material in the flux path [20, 21].

Building on this idea, consider the circuit in Figure 1(b), where a dependent current source has been added to the secondary circuit. Writing Kirchhoff's Voltage Law around the input loop gives

$$V_S = I_1 R_1 + j\omega L_1 I_1 + j\omega M I_2 = I_1 R_1 + j\omega \left(L_1 + \alpha M\right) I_1, \quad (2)$$

where we have taken the constant of proportionality between the secondary current and the primary current to be $\alpha = I_2/I_1$. In this case, the source sees the effective inductance $L_{eff} = L_1 + \alpha M$. Clearly this effective inductance can be negative if $\alpha < -L_1/M$. Further, the inductance can be continuously varied from enhanced positive values to negative values by varying α.
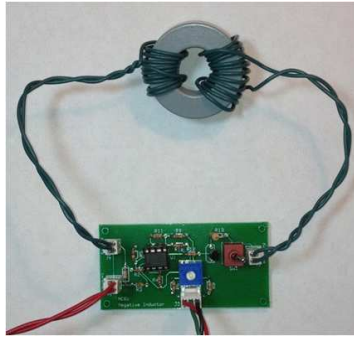
3. PROTOTYPE CIRCUIT

An active circuit for demonstrating the concept is shown in Figure 2. A small series resistor is used to sense the current in the input inductor winding. The voltage across this resistor is then amplified and used to drive a bipolar transistor output stage that serves as a voltage-to-current converter. For this circuit the effective value of α for time-varying signals is (see the Appendix)

$$\alpha = -\frac{\beta}{R_b}\frac{R_{f2}}{R_{i2}}\frac{R_{f1}}{R_{i1}}R_s. \qquad (3)$$

Using the values listed in Table 1, we obtain $\alpha \approx -7.64$. Measurements on the prototype circuit shown in Figure 3 were in reasonable agreement, with $\alpha \approx -7.08$. As shown in Figure 2, a DPDT switch was used with the secondary winding so that the effective α could be either negative, zero, or positive.
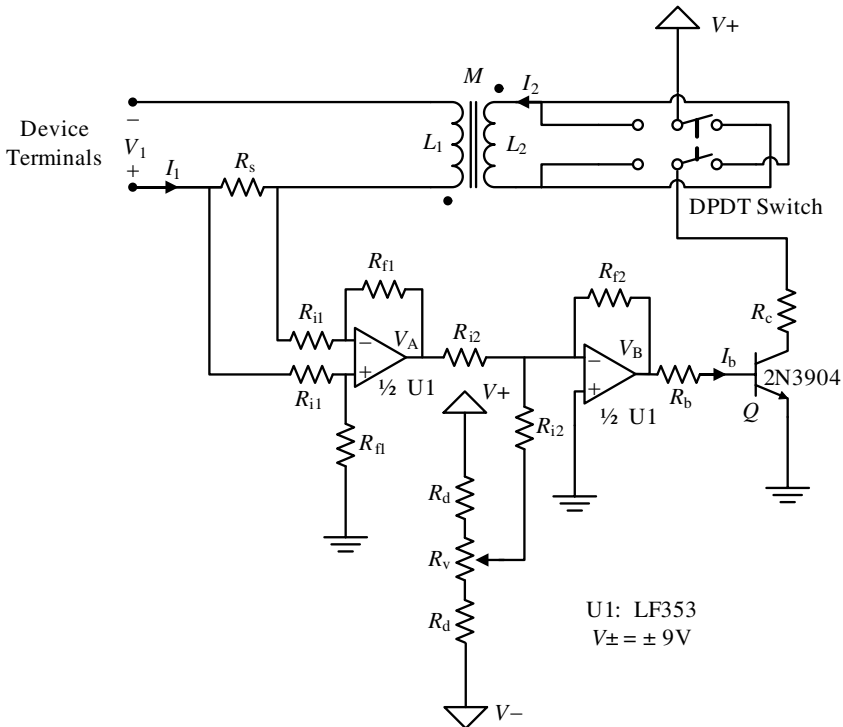
Figure 2. Circuit diagram for the prototype negative inductor. The DPDT switch is shown in the positive inductance position.

Figure 3. The prototype negative inductor circuit. The primary and secondary windings are to the upper left and right, respectively. The terminals to the effective component are at the lower left, and the power leads are shown at the bottom. The DPDT switch used to change the polarity of the secondary current is shown on the right of the circuit board next to the connector to the secondary winding.

An alternative to a series resistor for sensing the current is the use of a Hall Effect current probe. This approach may be of particular interest for applications in power electronics.

The coupled inductors were made using windings of #22 copper wire on an AMIDON FT-150A-K ferrite toroid. The primary (L_1) was formed with $N_1 = 10$ turns, and the secondary (L_2) was formed with $N_2 = 12$ turns. The self-inductance of each winding was inferred from the measured impedance as a function of frequency, and is listed in Table 1.

In all of the measurements reported here, the impedances were determined by measuring circuit voltages and their relative phases with a digital oscilloscope. For example the current was obtained by measuring the voltage across a series resistor, and the magnitude of the voltage across an inductor along with the measured phase difference with the current allowed the construction of a phasor representation of the voltage across the inductor. The impedance was then obtained by dividing the current into the phasor voltage.

Since an R-L circuit will be unstable if either R or L is negative, an additional series inductor was used to test the circuit. This inductor (L_0) was formed using 37 turns of #22 copper wire on a second FT-150A-K ferrite toroid. The simplified test circuit including L_0 and explicitly showing the current sense resistor R_s is shown in Figure 4.

Table 1. Component values used in the circuit shown in Figures 2 and 4.

Component	Value	Component	Value
R_s	$2.7\,\Omega$	R_1	$100\,\Omega$
R_{i1}	$10\,\text{k}\Omega$	β	283
R_{f1}	$100\,\text{k}\Omega$	L_0	$588\,\mu\text{H}$
R_{i2}	$1\,\text{k}\Omega$	L_1	$47.1\,\mu\text{H}$
R_{f2}	$4.7\,\text{k}\Omega$	L_2	$66.6\,\mu\text{H}$
R_b	$4.7\,\text{k}\Omega$	k	0.922
R_d	$4.7\,\text{k}\Omega$	$M = k\sqrt{L_1 L_2}$	$51.6\,\mu\text{H}$
R_v	$5\,\text{k}\Omega$	α (measured)	-7.08
R_c	$270\,\Omega$	τ (measured)	$1.12\,\mu\text{s}$
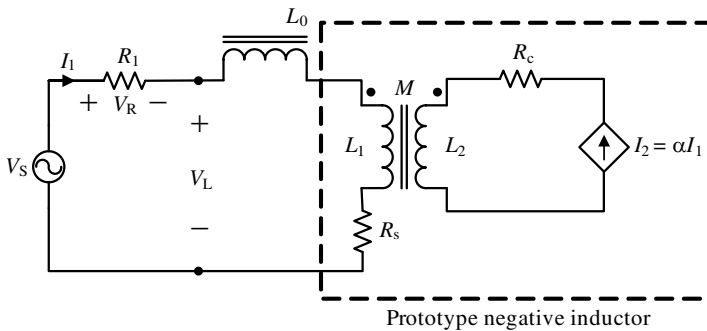
Figure 4. Circuit used to test the prototype negative inductor. The portion within the dashed lines is a simplified representation of the prototype circuit shown in Figures 2 and 3.

The impedance looking to the right at the terminals labeled V_L is

$$\frac{V_L}{I_1} = R_s + j\omega\left(L_0 + L_1 + \alpha M\right). \qquad (4)$$

In general, the realization of the dependent current source will be non-ideal, resulting in a phase shift other than 0 or 180 degrees. Thus we can write $\alpha = \pm|\alpha|\exp\left(j\phi_\alpha\right)$, where the sign is determined by the position of the DPDT switch feeding the secondary inductor, and the phase ϕ_α describes the departure from an ideal, zero-delay, dependent source. For the prototype of the circuit shown in Figure 2, a linear phase shift with frequency was measured corresponding to a constant delay through the circuit of about $\tau \approx 1.12\,\mu\text{s}$. The phase

shift can therefore be written $\phi_\alpha = -\omega\tau$. From (4), V_L also has a phase shift with respect to I_1, or $V_L = |V_L|\exp(j\phi_L)$. The real and imaginary parts of the impedance given by (4) can therefore be written (see also [12])

$$R_{eff} = \text{Re}\left\{\frac{V_L}{I_1}\right\} = \frac{|V_L|}{V_R}R_1\cos\phi_L = R_s \mp \omega\,|\alpha|\,M\sin\phi_\alpha$$
$$\approx R_s \pm \omega^2 M\,|\alpha|\,\tau, \tag{5}$$

and

$$\omega L_{eff} = \text{Im}\left\{\frac{V_L}{I_1}\right\} = \frac{|V_L|}{V_R}R_1\sin\phi_L = \omega\left(L_0 + L_1 \pm |\alpha|\,M\cos\phi_\alpha\right)$$
$$\approx \omega\left(L_0 + L_1 \pm |\alpha|\,M\right). \tag{6}$$

Here we have made the approximation $|\omega\tau| \ll 1$ in the second lines of Eqs. (5) and (6). This condition is satisfied for the frequency range under consideration.

If ϕ_α is close to 0 or π, then the main effect is to modify the inductance. In contrast, if ϕ_α is close to $\pi/2$, then the main effect is to modify the resistance. The latter case has been the focus of techniques to enhance the Q of an inductor [9–12], while we here concentrate on the former case. As we shall see, for small negative values of ϕ_α, it is
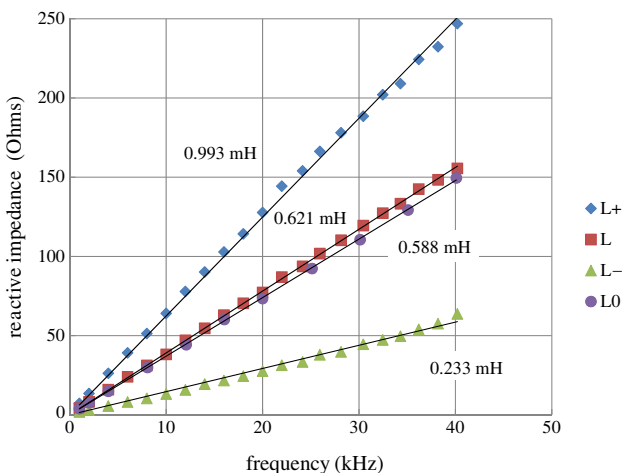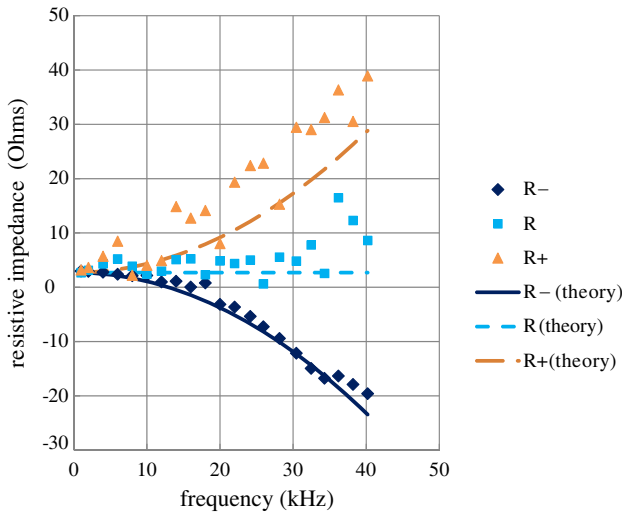

Figure 5. Reactive impedance measured at the terminals labeled V_L in Figure 4. $L+$, L, $L-$ correspond respectively to the enhanced, passive, and negative inductance positions of the DPDT switch controlling the current phase in the secondary. L_0 corresponds to the impedance of the reference inductor alone.

possible to simultaneously achieve negative inductance and improved Q.

The real and imaginary parts of the measured impedance are shown in Figures 5 and 6. The data points shown were obtained using measured values of V_L and V_R along with the first expressions in Eqs. (5)and (6). The trend lines in the reactive impedance (Figure 5) are the result of linear fits to the data. The curves are labeled with the inductance values obtained from the slopes. These values are in reasonable agreement with evaluations of the right-hand-side of Eq. (6) using the values given in Table 1. Note that since $|\alpha| M > L_1$, the effective value of the active inductor becomes negative when the secondary coil is connected with the appropriate phase, thus reducing the total effective inductance to a value below L_0. The value of the effective negative inductance is $0.233 - 0.588 = -0.355\,\mathrm{mH}$. The effective inductance in the enhanced mode is $0.993 - 0.588 = 0.405\,\mathrm{mH}$.

The solid curves for the resistive impedance (Figure 6) were computed using the last expression in (5) along with the component values listed in Table 1. The scatter in the measured points for the R and $R+$ curves results from the difficulty of measuring the small value of resistance in the presence of the much larger reactance (8 to 55 times larger). In contrast, the scatter is much smaller for the $R-$ curve

Figure 6. Resistive impedance measured at the terminals labeled V_L in Figure 4. $R-$, R, $R+$ correspond respectively to the negative, passive, and enhanced inductance positions of the DPDT switch controlling the phase of the current in the secondary.

since in this case the resistance is as much as $\sim 40\%$ of the reactance. Note that the phase shift from the small delay through the amplifier causes a negative contribution to the resistance when the inductance is negative. This contribution dominates for the higher frequencies resulting in a net negative effective resistance. For frequencies in the range of 10–12 kHz, the effective resistance of the negative inductor is close to zero, resulting in an enhanced component Q. The total effective series resistance in the input loop remains positive, however, owing to the presence of R_1 as well as the internal impedance of the source (not shown in the diagram).

4. SUMMARY

In summary, an active circuit presenting a negative inductance has been described, and demonstrated over the frequency range 1 to 40 kHz. This component differs from previous realizations using negative impedance converters in that the inductance is realized using physical magnetic flux. By varying the gain and polarity of an incorporated current amplifier, the effective inductance can be varied over both negative and positive values. Adjusting the phase of the current amplifier can also introduce negative resistance that can counter ohmic loss, improving the effective Q of the inductor. The new component also fails gracefully, in that if the dependent current source in Figures 1 and 4 were to fail as either an open or short circuit, the component will behave as an ordinary passive inductor.

APPENDIX A.

The outline of the derivation of Eq. (3) is as follows. The voltage drop across the current sensing resistor R_s is $I_1 R_s$, assuming the input impedance of the differential amplifier is much larger than that of the sensing resistor ($2R_{i1} \gg R_s$). Referring to the values in Table 1, this assumption is well-satisfied. (The use of an instrumentation amplifier would be ideal, but at the cost of two additional voltage follower amplifiers. In the present case, this additional complexity was not warranted.) The output of the input differential amplifier stage is therefore

$$V_A = \frac{R_{f1}}{R_{i1}} R_s I_1. \tag{A1}$$

The output of the following inverting amplifier is $V_B = -(R_{f2}/R_{i2})V_A$, or

$$V_B = -\frac{R_{f2}}{R_{i2}} \frac{R_{f1}}{R_{i1}} R_s I_1. \tag{A2}$$

Neglecting the small-signal input resistance of the output transistor Q, the base current is $I_b = V_B/R_b$. With the DPDT switch in the left position, the collector current is $I_2 = \beta I_b = \beta V_B/R_b$. Combining this result with Eq. (A2) and solving for the ratio $\alpha = I_2/I_1$ leads to Eq. (3).

REFERENCES

1. Foster, R. M., "A reactance theorem," *Bell Syst. Tech. J.,* Vol. 3, 259–267, 1924.

2. Merrill, J. L., "Theory of the negative impedance converter," *Bell Sys. Tech. J.*, Vol. 30, 88–109, Jan. 1951.

3. Linvill, J. G., "Transistor negative impedance converters," *Proc. IRE*, Vol. 41, 725–729, Jun. 1953.

4. Kuo, C. K. and K. L. Su, "Some new four terminal NIC circuits," *IEEE Proc. Circuit Theory*, 379–381, Aug. 1969.

5. Sussman-Fort, S. E., "Gyrator-based biquad filters and negative impedance converters for microwaves," *Int. J. RF Microw. Comput.-aided Engr., (Special Issue on Net. Synthesis Method. Microw. Dev.)*, Vol. 8, No. 3, 86–101, Mar. 1998

6. Antoniou, A., "Floating negative impedance converters," *IEEE Trans. Circuit Theory*, Vol. 19, No. 2, 209–212, Mar. 1972.

7. Sussman-Fort, S. E. and R. M. Rudish, "Non-foster impedance matching of electrically-small antennas," *IEEE Trans. on Ant. and Prop.*, Vol. 57, No. 8, 2230–2241, Aug. 2009.

8. Yuan, Y., B.-I. Popa, and S. A. Cummer, "Zero loss magnetic metamaterials using powered active unit cells," *Optics Express*, Vol. 17, No. 18, 16135–16143, Aug. 31, 2009.

9. Pehlke, D. R., A. Burstein, and M. F. Chang, "Extremely high-Q tunable inductor for Si-based RF integrated circuit applications," *Proc. IEDM*, 63–66, Washington, D.C., Dec. 1997.

10. Georgescu, B., H. Pekau, J. Haslett, and J. McRory, "Tunable coupled inductor Q-enhancement for parallel resonant LC tanks," *IEEE Trans. Circuits and Systems — II: Analog and Digital Sig. Proc.*, Vol. 50, No. 10, 705–713, Oct. 2003.

11. Saha, P. K., A. Dutta, T. K. Bhattacharyya, and A. Patra, "Effects of active Q enhancement on oscillator phase noise: An analysis," *Analog Integr. Circ. Sig. Process*, Vol. 52, 99–107, 2007.

12. Cusmai, G., M. Repossi, G. Albasini, A. Mazzanti, and F. Svelto, "A magnetically tuned quadrature oscillator," *IEEE Journal of Solid-State Circuits*, Vol. 42, No. 12, 2870–2877, 2007.

13. Yue, C. P. and S. S. Wong, "On-chip spiral inductors with patterned ground shields for Si-based RF IC's," *IEEE Journal of Solid State Circuits*, Vol. 33, No. 5, 743–752, May 1998.

14. Decanis, U., A. Ghilioni, E. Monico, A. Mazzanti, and F. Svelto, "A low-noise quadrature VCO based on magnetically coupled resonators and a wideband frequency divider at millimeter waves," *IEEE Journal of Solid-State Circuits*, Vol. 46, No. 12, 2943–2955, Dec. 2011.

15. Groves, R. A. and D. K. Jadus, "Switched inductor/varactor tuning circuit having a variable integrated inductor," US Patent No. 6,549,096, Apr. 15, 2003.

16. Rais-Zadeh, M., P. A. Kohl, and F. Ayazi, "MEMS switched tunable inductors," *Journal of Microelectromechanical Systems*, Vol. 17, No. 1, 78–84, 2008.

17. Demirkan, M., S. P. Bruss, and R. R. Spencer, "Design of wide tuning-range CMOS VCOs using switched coupled-inductors," *IEEE Journal of Solid-State Circuits*, Vol. 43, No. 5, 1156–1163, 2008.

18. Kossel, M., T. Morf, J. Weiss, P. Buchmann, C. Menolfi, T. Toifl, and M. L. Schmatz, "LC PLL with 1.2-octave locking range based on mutual-inductance switching in 45-nm SOI CMOS," *IEEE Journal of Solid-State Circuits*, Vol. 44, No. 2, 436–449, 2009.

19. Wen, C.-Y., E. K. Chua, R. Zhao, T. X. Chong, J. A. Bain, T. E. Schlesinger, L. T. Pileggi, and J. Paramesh, "A phase-change via-reconfigurable on-chip inductor," *Proc. 2010 IEEE International Electron Devices Meeting (IEDM)*, 10.3.1–10.3.4, Dec. 6–8, 2010.

20. Salvia, J., J. A. Bain, and C. P. Yue, "Tunable on-chip inductors up to 5 GHz using patterned permalloy laminations," *IEEE International Electronic Devices Meeting (IEDM) Technical Digest*, 943–946, Dec. 2005.

21. Ning, N., X. P. Li, J. Fan, W. C. Ng, Y. P. Xu, X. Qian, and H. L. Seet, "A tunable magnetic inductor," *IEEE Trans. Magnetics*, Vol. 42, No. 5, 1585–1590, May 2006.